Development of Analytical Strategies to Optimize the Use of Photovoltaic Water Pumping Systems: An optimization approach

Thomas Florian Pötzl
thomas.potzl@tecnico.ulisboa.pt

Instituto Superior Técnico, Universidade de Lisboa, Portugal

October 2023

Abstract

The introduction of solar-powered water pumping systems has become a viable alternative for farmers for irrigation and water supply around the world. However, access to water in the most remote areas of the world is limited. To ensure a reliable water supply, solar-powered water pumping systems need to be efficient and sustainable. This study examines the development of analytical strategies to maximize the effectiveness of the use of photovoltaic systems in water pumping systems. As a result, the study focuses on developing accurate models of the subsystems of solar-powered water pumping systems. The goal is to have reliable models in order to obtain the best subsystem efficiency solutions. Therefore, a model for the simulation of photovoltaic arrays and the motor-pump unit is developed and implemented in a Matlab environment. When the behavior of the subsystems is accurately modeled, it is possible to prioritize and maximize the total efficiency of the system by the correct choice of components. However, the comparative analysis showed that the efficiency is strongly related to the environmental circumstances of the investigated locations. As a consequence, not every location is suitable for standalone solar-powered water pumping systems and potentially needs a backup power source to avoid oversizing the photovoltaic array. In addition to the critical analysis of the results, potential bottlenecks, such as space and location constraints, are identified. On the basis of this analysis, tasks for future work and potential extensions of the models and the methodology are introduced.

Keywords: PV water pumping, Solar-based water pumping system, Irrigation, Energy efficiency

1. Introduction

The United Nations has set an important objective: to ensure the availability and sustainable management of water and sanitation for all people around the world. This imperative has become a pressing global issue driven by population growth, ongoing urbanization, and the growing demand for water from agriculture and other sectors. These trends have led to the unfortunate reality that billions of people do not have access to clean water. The challenges associated with water scarcity are further compounded by climate change [14]. This is of great concern because freshwater plays a crucial role in the maintenance of the health of ecosystems and is essential for human survival [11].

The role of Solar-Powered Water Pumping Systems

Three different questions arise: How is it possible to ensure access to fresh water even in the world's most remote areas? How is it possible to do so in an environmentally friendly way to mitigate the impacts of climate change? How can this be applied to the agricultural sector as one of the drivers of water scarcity and climate change?

A promising answer to these questions may be the role of solar-powered water pumping systems. To enable access to water in the most remote areas in the world where water is still needed, solar-powered water pumping systems can help. These remote areas of the world usually have limited access to electricity, so solar-powered water pumping systems have become an important factor in ensuring fresh water supply [17]. In addition, solar energy is an abundant and environmentally friendly energy source, available almost everywhere throughout the world [15].

The environmental benefit of using solar-powered water pumping systems is connected to the global energy transition effort, leading to an exponential expansion of renewable energy sources worldwide. Consequently, by using a renewable source

to power the water supply, the effects of climate change can be mitigated [18]. In agriculture worldwide, irrigation is a well-established and necessary practice [15]. However, agriculture is considered one of the main water users on a global scale. According to [16], the question of sustainability in agriculture has become more prominent in recent years in research [16].
The introduction of solar-powered water pumping systems may be a viable alternative for farmers. This technology increases the efficiency of water use while simultaneously contributing to socio-economic development [15]. The research question is addressed by developing analytical strategies to optimize the use of photovoltaic systems in water pumping systems.
As a result, the study focuses on developing accurate models of the subsystems of solar-powered water pumping systems, enabling us to prioritize and optimize the total efficiency of the system. In detail, this means to implement an accurate model for the photovoltaic array and motor-pump unit in Matlab. By linking both models, it is possible to obtain an optimized component selection algorithm that focuses on maximizing the energy efficiency from the source of energy to the actual use of water.

2. Design parameters

2.1. Water demand

The water demand and the corresponding water output Q are a design parameter that must be known or estimated in advance [6].The height that the pump must overcome is referred to as the total dynamic head (TDH) and can be described as:

$$TDH = \text{Static Head} + \text{Discharge Head} + \text{Friction Head} \quad (1)$$

This is the total of the static head, the discharge head, and the head losses due to friction [13] [10]. The static head is the vertical distance to the source depth. The discharge head describes the vertical distance above ground level to the storage tank that, when elevated, allows use through gravity. The friction head describes the friction of the water against the insides of the pipes. It usually represents 10% of the static head plus the discharge head [19].

2.2. Hydraulic system - Motor-pump unit

The hydraulic energy required for a specific water demand and total dynamic head is given by [6]:

$$P_H = Q \cdot TDH \cdot \rho \cdot g \quad (2)$$

where Q = water flow rate (m^3/h), TDH = total dynamic head (m), ρ = liquid density, in this case water density (1000 kg/m^3), g = gravity acceleration ($9.81 m/s^2$). Using this equation, we can accurately estimate the power requirements for a pumping system to meet specific water demands, allowing us to select appropriate pumps and optimize the system's efficiency. For a centrifugal pump, the relationship of parameters that result in pump efficiency is determined by the following.

$$\eta_{\text{pump}} = \frac{P_H}{P_{\text{pump in}}} = \frac{Q \cdot H \cdot \rho \cdot g}{P_{\text{pump in}}} \quad (3)$$

where $P_{\text{pump in}}$ = pump input power (W) and H = TDH (m) [3]. The pump input power describes the mechanical input power from the electrical machine to the pump, which then further describes the relationship between the hydraulic output power and the mechanical input power as the pump efficiency:

$$\eta_{\text{pump}} = \frac{P_H}{P_{\text{m in}}} \quad (4)$$

where P_p = hydraulic output power (W) and $P_{\text{m in}}$ = mechanical input power (W) [12]. The pump's efficiency is a critical factor in assessing the pump's performance and is an important consideration in pump selection and system design. Higher pump efficiency indicates better energy utilization and reduced losses in the pumping system.
The motor-pump unit is then determined by introducing the efficiency of the electrical machine. It is represented as the following:

$$\eta_{\text{EM}} = \frac{P_{\text{m out}}}{P_{\text{sup}}} = \frac{P_{\text{m out}}}{I_o \cdot V_o} \quad (5)$$

where $P_{\text{m out}}$= mechanical output power which is equal to P_{shaft}, P_{sup} = supplied power by the photovoltaic array (or power converter - depending on configuration), I_o = output current (A) and V_o = output voltage (V) [9]. The formula considers both the mechanical and electrical output power. It helps us to evaluate the effective utilization of the energy generated by the photovoltaic array to achieve the desired mechanical output power on the pump shaft.

2.3. Power converter

Depending on the system configuration, a power converter must be introduced. To obtain the energy losses, the efficiency can be described as [5] (modified nomenclature):

$$\eta_i = \frac{P_{\text{out}}}{P_{\text{DC}}} \quad (6)$$

with P_{out} = output power (W), P_{DC} = input power (W). The efficiency of the converter η_i connects the input power of the photovoltaic array to the output power of the converter [5]. In solar-powered pumping applications, the efficiency of the power converter affects overall energy utilization and system performance.

2.4. PV array

Solar irradiation G is the solar radiation per unit of area, often described in $W/m^2/day$. It results from solar irradiance G (W/m^2), which shows the rate at which the radiant energy is incident to the surface area over time. Total solar radiation is also called global radiation on a horizontal surface. It includes beam radiation, solar radiation without the effect of scattering in the atmosphere, and diffuse radiation, which describes radiation received after a direction change due to scattering of the atmosphere[8]. Solar irradiance varies as the position of the Sun to the surface changes over the day. Solar insolation can also be described as sun peak hours. Several influences affect solar irradiance on the photovoltaic array, including latitude, atmospheric clarity, humidity, and seasonal variations[19].

The photovoltaic power output is directly dependent on the irradiance and the temperature of the cell. Power output varies according to the operating point, which is the main parameter for the efficiency of the photovoltaic systems. This means that the output power of the photovoltaic array can be characterized to [5]:

$$P(G,T) = \frac{G}{G^r} \cdot P_{\mathsf{p}} \cdot [1 + \mu_{P_p} \cdot (T - T^r)] \qquad (7)$$

where P_p = peak power corresponding to maximum DC power output (W_p), μ_{P_p} = peak power temperature coefficient (% / ºC), G^r = irradiance at standard conditions (STC) G^r = 1000 (W/m^2), T = current cell temperature (K) and T^r = temperature at STC cell temperature $\theta_m^r = 25$ ℃ (K). To obtain the needed current temperature of the cell, the relationship of normal operation cell temperature, the irradiance (G), and the ambient temperature (T_{amb}) is given as [5] :

$$T_{\mathsf{cell}} = T_{\mathsf{amb}} + G \cdot \frac{NOCT - 20}{800} \qquad (8)$$

where T_{cell} = cell temperature (K) and T_{amb} = ambient temperature (K). Normal operation cell temperature (NOCT) is usually a parameter provided by the manufacturer in the solar panel datasheet. This method is a simplified approach to estimating the panel temperature and influence on the power output at a given operating point. The Ross model has shown that this method is an approximation and shows some errors compared to the experimental data [5].

To be able to compute the overall efficiency of the system, the photovoltaic array efficiency is described as:

$$\eta_{\mathsf{pv}} = \frac{I_o V_o}{G A_{\mathsf{pv}} n_s n_p} \qquad (9)$$

where n_s = cells connected in series (n), n_p = cells connected in parallel (n), V_o = output voltage (V) and I_o = output current (A) [9]. The resulting efficiency of the panel can then be simplified to:

$$\eta_{\mathsf{pv}} = \frac{P(G,T)}{G \cdot A_{\mathsf{pv}}} \qquad (10)$$

This equation establishes a connection between the output power, P (G,T), derived from the output voltage V_o and output current I_o and the solar irradiance per unit area of the PV array [5].

The efficiency of the photovoltaic array is a crucial parameter in determining the efficiency with which sunlight radiation is converted into electrical energy and is an essential factor in the calculation of the overall efficiency of a solar-powered water pumping system. By maximizing the efficiency of the photovoltaic array, more electrical power can be generated from the available solar energy, contributing to the overall effectiveness of the system.

2.5. Summary

By combining the efficiencies of the photovoltaic array of Equation 9 with the efficiency of the electrical machine in Equation 5 and the efficiency of the pump in Equation 3, we have a total efficiency of the system of solar-powered water pumping systems:

$$\eta_{\mathsf{total}} = \eta_{\mathsf{pv}} \cdot \eta_{\mathsf{EM}} \cdot \eta_{\mathsf{pump}} \qquad (11)$$

when there is no power converter involved [9]. When there is a power converter present, then Equation 11 is added by Equation 6, which allows us to obtain the total efficiency of the system, including all subsystems:

$$\eta_{\mathsf{total}} = \eta_{\mathsf{pv}} \cdot \eta_{\mathsf{EM}} \cdot \eta_{\mathsf{pump}} \cdot \eta_{\mathsf{i}} \qquad (12)$$

This formula describes the ratio of hydraulic power output to the input solar power [7].

The main objective of optimizing the total efficiency of the system is to achieve the maximum hydraulic power output using the available solar power input by selecting suitable components.

3. Methodology

After establishing the parameters of the subsystems, the design and choice of components are possible. However, to optimize the photovoltaic water pumping system, it is mandatory to prioritize the efficiency of the system. It is possible to create and introduce operating ranges of the system when the water demand is unknown. This means that all possible combinations of motor-pump units connected to a photovoltaic system can be identified. The fixed variable for the photovoltaic array will be the location, including temperature and irradiance. For the motor pump unit, the total dynamic head must be known to identify all possible pumps. Figure 1 shows the proposed methodology

considered for this work for the development of the different operating ranges of the photovoltaic water pumping system.

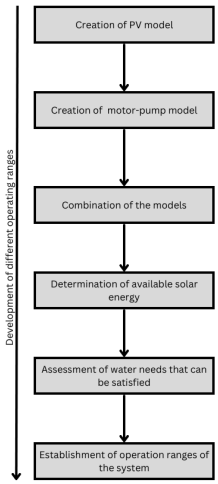

Figure 1: Flowchart for the development of different operating ranges for the photovoltaic water pumping system

4. Implementation

4.1. Proposed PV model

One-diode five-parameter model

The electrical model used is shown in Figure 2. The model referred to is commonly known as the one-diode five-parameter model, also known as the single-diode model with five parameters. The one-diode five-parameter model is a widely used approach in the modeling of photovoltaic systems and takes into account the various losses present in a PV panel [5].

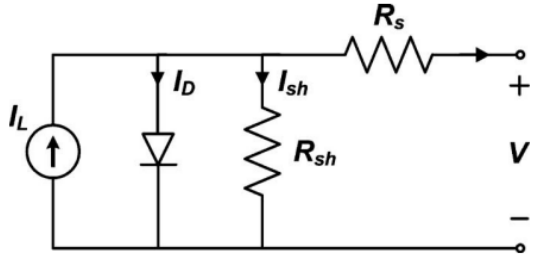

Figure 2: Equivalent circuit of the photovoltaic solar cell used in the 1 Diode 5 parameter model from [4]

The relationship of the current and the voltage in a solar panel is given as [5] (Equation has been modified due to nomenclature):

$$\begin{aligned} I &= I_L - I_D - I_{\text{sh}} \\ &= I_L - I_o \left[\exp\left(\frac{V + IR_s}{a \cdot Vt} \right) - 1 \right] - \frac{V + IR_s}{R_{\text{sh}}} \end{aligned} \tag{13}$$

where I = operation current, I_L = light current (A), I_D = diode current (A), I_{sh} = shunt current (A), I_o = saturation current (A), R_s = series resistance (Ω), R_{sh} = shunt resistance (Ω), vt = thermal voltage (V) and a = diodes ideality factor (-). The goal of the model is to retrieve the individual I-V and P-V curves of the different panels, as shown in the datasheet of the photovoltaic panel. An I-V curve is a graphical representation of a PV panel's current and voltage relationship, whereas the P-V curve shows the relationship between the output power and the corresponding voltage. When the characteristic curves are obtained, it is possible to identify the operating points with a given irradiance and temperature. The ultimate goal is to intersect the operating points of both the PV panel and the motor-pump unit to maximize the efficiency between the components. The flow chart that illustrates the implementation process is presented in Figure 3. The methodology comprises six distinct steps, which form a well-defined algorithm to extract the characteristic curves of various PV panels under varying environmental conditions.

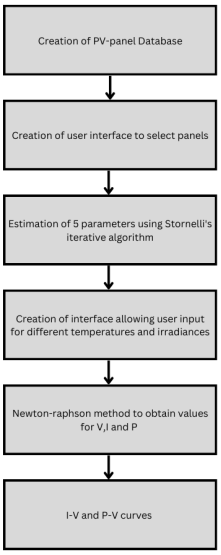

Figure 3: Flowchart of the implementation into Matlab

4.2. Proposed Motor-pump model

Overview and Flowchart

The two input parameters of the model are height H and Outflow Q. These two parameters enable us to create the operation ranges in which the motor-pump combinations show the highest efficiency. Parallelly, another input of the model is the digitized data provided by the manufacturer. This step includes the import of PQ and HQ curves, tables that connect each pump to a corresponding motor, and the motor data itself. The next task is to connect the input parameters with the given data to identify possible motor-pump combinations for the user's requirements. Here, the data between the

characteristic curves and the tables are matched. As an output, we obtain all possible outflows Q and powers P that satisfy the height. Here, the user input height is the mandatory pressure requirement of the system. This means that the outflow Q will be a variable parameter possibly higher or lower than the user's input. Afterward, with the pump efficiency at the operating outflows, it is possible to identify the load on the motor. Interpolating the efficiencies with the load on the motor, we will obtain the power the motor absorbs with the highest efficiency motor-pump combination. This is the power that the motor demands from the source, the photovoltaic supply, enabling us to connect the two models. The final output displays all possible combinations in case the user prefers to choose a different motor-pump combination, not prioritizing the highest efficiency. A visualization of the flowchart of implementation is shown in Figure 4.

Figure 4: Flowchart of developing motor-pump model

4.3. The PV / Motor-pump coupling model

Figure 5 shows an overview of the system, where all input parameters are shown in light blue. The power converter is not particularly modeled. As it is an important part of the system, an assumption of constant efficiency is made. Referring back to Equation 6, the following assumption is made:

$$\eta_i = 95 - 98\% \tag{14}$$

This assumption represents all components, which allows the calculation of all system parameters. In doing so, different operating ranges can be established, meaning for different locations and water supply demands.

5. Experimental Work

5.1. Example system 1, Azoia de Baixo, Portugal

The system to evaluate the methodology consists of a photovoltaic array, an inverter, a motor-pump set, and additional components such as wiring and piping. The example system is located in the area of Azoia de Baixo, Portugal, as it can be seen in Figure 6.

Figure 6: Location of example system 1 [1]

5.1.1 Motor-pump unit

For choosing the ideal motor-pump unit, we need to consider the total dynamic head with the input H and amount of wanted outflow Q. As for the water source, we are considering a well system that results in the use of a submersible motor pump unit. For this case study, we validate the model with the following input parameters:

Table 1: Azoia de Baixo - Daily average water needs

Month	Water need (m^3/day)
Jan.	10
Feb.	15
Mar.	19
Apr.	21
May	33
Jun.	35
Jul.	40
Aug.	33
Sep.	24
Oct.	18
Nov.	10
Dec.	9

Parameter H describes the total dynamic head. For this case study, we assume the total pressure of the system to H = 100 m. Table 1 gives us insight into the water consumption pattern of the selected location by showing the average daily outflows needed for each month. Given this information, we have the necessary input for the motor-pump model. The motor-pump model with the given input creates the following outputs, as seen in Table 2 and Table 3.

The result shows all possible combinations of motor-pump units satisfying the input of H = 100m. The selected location does not require a fixed outflow per hour, which means that to select the best-suited pump, we consider the best subsystem efficiency of the combined motor-pump unit.

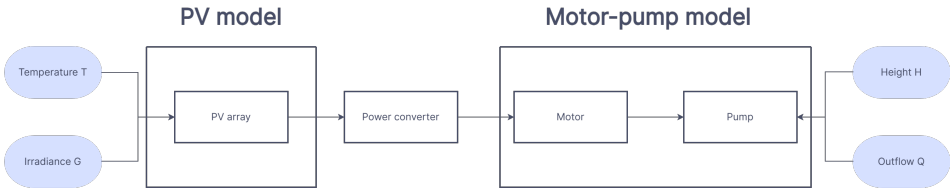

Figure 5: Overview of system

This means that the pump SP7_27 with the motor MS 4000 is selected showing a motor efficiency of $\eta_{\text{Motor}} = 78.24\%$ and a pump efficiency of $\eta_{\text{Pump}} = 66.82\%$ resulting in the highest subsystem efficiency of $\eta_{\text{subsystem}} = 52.28\%$. To ensure the supply of 8.19 m^3h^{-1}, the motor absorbs a power of 4340 W that must be supplied by the photovoltaic array.

5.1.2 Power Converter/Controller

The power converter efficiency must be considered to calculate the power needed for the photovoltaic system. As stated in Equation 14, the efficiency of the power converter is assumed to be between 95% and 98%, resulting in a power supply of:

$$P_{\text{Needed}} = \frac{P_{\text{Motor}}}{0.98} = 4428.6W \tag{15}$$

An alternating current converter is required for this representative system because the pumps are alternating current pumps. In this context, it is important to note that although a detailed modeling of the power inverter is not within the scope of this study, we assume constant efficiency for the selected inverter. The power converter selection process involves a comprehensive validation procedure.

5.1.3 Photovoltaic array

Radiation data

After introducing the possible setup, defining the available solar resources is necessary. Azoia de Baixo (Latitude: 39.303, Longitude: -8.711) is the example location. The available solar radiation and the dry bulb temperature can be taken from the PVGIS website [2]. The average ambient temperature is presented in Figure 7a and the global horizontal irradiance in Figure 7b.

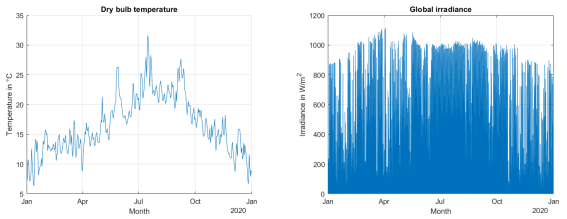

(a) Dry bulb temperature **(b)** Global horizontal irradiance

Figure 7: Azoia de Baixo - Data retrieved from PVGIS

With information on dry bulb temperature and global horizontal irradiance, we can conclude the cell temperature and, ultimately, the loss of efficiency according to Equation 8 and Equation 10 using the photovoltaic model.

Time of pump usage

The needed time the power is demanded is determined by the water needed per day divided by the pump's outflow for the fixed and given height. This means for July:

$$Time_{\text{July}} = \frac{40m^3/day^{-1}}{8.19m^3h^{-1}} = 4.88h \tag{16}$$

In July the pump has to run 4.88 hours to satisfy the needed $40m^3/day$. The results for each month of the year are summarized as a part of Table 4.

Analysis

To validate the desired system, we calculate a factor that indicates the month with the highest relation between the needed energy and the available energy. This step is the first estimation to identify the design's worst case, the relevant case. Table 4 shows the pattern of water demand paired with the amount of irrigation time, resulting in a daily energy value needed when multiplying the number of hours with the power needed by the pump of 4428.6 W. This energy is then compared to the peak sun hours obtained per day. Peak sun hours describe the number of hours during one day when the insolation averages an equivalent solar irradiance of 1000 W/m^2 [18]. Given this information, it is possible to calculate a factor by dividing the needed energy by the equivalent sun hours, indicating the relevant month for the design. In this case, July shows the highest value. As a consequence, a typical day in July is analyzed to obtain the correct design of the photovoltaic system.

Results

It is possible to calculate the number of needed panels by the following equation:

$$N_{\text{panel}} = \frac{P_{\text{Load}}}{P_{\text{DC}}} \tag{17}$$

where $P_{\text{Load}} = 4428.6W$. Given the fluctuating power supply of the photovoltaic panel, the number of panels needed varies for each irradiance value. The approach divides the needed load P_{Load} by the power that one panel generates throughout the day. As a result, we obtain the number of panels needed for the specific irradiance to achieve the power needed for the required time. To conclude the number of panels needed, the time when we can satisfy the water supply is considered. Therefore, it is investigated for how long the photovoltaic array configuration can provide the required input power. Applying the approach for a typical day in July with the representative photovoltaic panel LC-50-12M, we need to satisfy the outflow for 4.88h, resulting in a minimum number of panels of 114. As a comparison in December, we need the minimum number of panels of 98 to satisfy the outflow of $8.19m^3h^{-1}$ for 1.10h. To enable usage throughout the year, the setup for the highest number of the worst-case scenario is chosen. Comparison between December and July showed that considering December would lead to an undersized photovoltaic array. As a result, the necessary power supply and therefore the required water demand could not be satisfied. The results for all panels of the database are shown in Table 5. The table gives information about the systems and their total efficiency. The Solar Panel A-270P shows the highest overall system efficiency of 8.38%, according to the calculation:

$$\begin{aligned}\eta_{\text{total}} &= \eta_{\text{pv}} \cdot \eta_{\text{EM}} \cdot \eta_{\text{pump}} \cdot \eta_{\text{inv}} \\ &= 16.36\% \cdot 78.24\% \cdot 66.82\% \cdot 98.00\% \\ &= 8.38\% \end{aligned} \tag{18}$$

The selection of this system with the highest efficiency necessitates using 22 panels, yielding a system's peak power output of 5940 W and requiring an area of 35.72 m^2.

5.2. Example system 2, Marzling, Germany

As a second location, the suburban village of Marzling is chosen. Marzling is a small village close to the metropolitan region of Munich and is suitable for the case study because of its agricultural activities. The location of the researched area is shown in Figure 8.

Figure 8: Location of example system 2 [1]

5.2.1 Motor-pump unit

We use the same input parameters for the second system to compare the influence of the location on the design and the sizing of the solar-powered water pumping system. This means that the output of the motor-pump model is equal to Table 2 and Table 3. Also the water demand is equal to Table 1. Therefore, the chosen motor-pump unit is the highest efficiency combination, the pump SP7_27 paired with the submersible motor MS 4000. The parameters resulting are an absorbed power by the motor of $P_{\text{Motor}} = 4340W$ and an outflow $Q = 8.19m^3h^{-1}$, which must be supplied by the photovoltaic array.

5.2.2 Power Converter/Controller

Again, the power efficiency of the converter must be considered to calculate the power needed for the photovoltaic system resulting in a power supply of:

$$P_{\text{Needed}} = \frac{P_{\text{Motor}}}{0.98} = 4428.6W \tag{19}$$

5.2.3 Photovoltaic array

The data again is retrieved from the PVGIS website [2]. The location is at latitude: 48.413, longitude: 11.797. The characteristic dry bulb temperature can be found in Figure 9a and the global horizontal irradiance in Figure 9b.

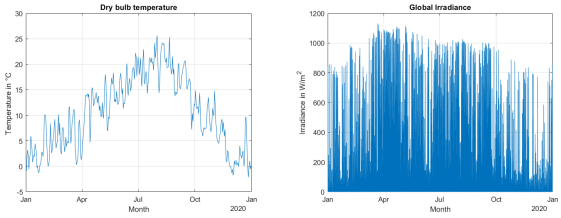

(a) Dry bulb temperature **(b)** Global horizontal irradiance

Figure 9: Marzling - Data retrieved from PVGIS

Analysis

We calculate the factor that indicates the month with the highest relationship between the energy needed and the energy available. Table 6 shows the pattern of water demand paired with the amount of irrigation time, resulting in a daily energy value when multiplying the hours by the power needed by the pump of 4428.6 W. This energy is then compared to the peak sun hours obtained per day. In this case, December shows the highest factor with 6.33, the month to consider for designing and sizing the photovoltaic array.

Results

When analyzing the month of December with the panels available from the database, it becomes clear that the number of panels needed increases significantly for all types of individual panels. The results of the modeling with the tool are summarized in Table 7. The efficiency of the panel is mostly lower than standard conditions (STC) efficiency and the efficiency of the previously researched location. This is because of the non-ideal conditions in operation where the ambient temperature is very low. Correction of electrical performance due to the low cell temperature benefits the overall efficiency of the panel during operation, but because the irradiance is noticeably lower than in standard conditions, the overall efficiency of the panel in operation decreases. The system with the highest efficiency can be observed with the Panel A-270P and is calculated as:

$$\begin{aligned} \eta_{\text{total}} &= \eta_{\text{pv}} \cdot \eta_{\text{EM}} \cdot \eta_{\text{pump}} \cdot \eta_{\text{inv}} \\ &= 13.79\% \cdot 78.24\% \cdot 66.82\% \cdot 98.00\% \\ &= 7.07\% \end{aligned} \tag{20}$$

This system needs $N = 130$ panels to satisfy the required power for the demanded time of operation, resulting in a peak power P_{Peak} of 35100W and an area of 210.6 m^2.

6. Comparison of results

The comparison between the results of system 1 and system 2 serves to highlight the difference in external parameters. To compare the final results, the best system efficiencies of both systems are presented in Table 8. When comparing the results for system 1 and system 2 it becomes noticeable that the size of the photovoltaic array is strongly linked to the location. For the same water output and required total dynamic head system 2 in Marzling has to be sized almost 6 times bigger in peak power than in Azioa de Baixo. This results in a much larger space utilization of up to 210 square meters. Additionally, there is a significant drop in efficiency when comparing the two locations. The efficiency of the photovoltaic array in Azoia de Baixo is of 16.36% compared to 13.79% in Marzling, resulting in a total system efficiency of 8.38% versus 7.07%. There are several probable reasons for this observation. The irradiance received in Azoia de Baixo is significantly higher than the irradiance received in Marzling over a year. As a consequence, the photovoltaic array has to be extremely oversized, making it a nonviable option for a standalone system in the area of Marzling. In this scenario, a complementary power source, such as a grid supply, would be needed. In contrast, the combination of components found for Azoia de Baixo appears to be a viable option for the required water demand and total dynamic head, resulting in a peak power of the system of only 5940 W and utilizing only a space of 35.72 m^2. The peak power in comparison does not exceed the power supply of 4428.6 W needed by a large margin.

Since this research focuses on efficiency, the general observation can be made that the photovoltaic panels with the best individual efficiency also show the best efficiency during operation. This does not necessarily mean that the panel with the highest efficiency will be the solution with the least space utilization or the solution that is the most economical. This issue will be discussed later as it comes to the limitations and future work of this research.

7. Conclusions

Ultimately, the research on the optimization of solar-powered water pumping systems has shown an interesting approach to optimize the usage of such systems. With the introduction of a motor-pump model, it was possible to identify the best combination of components between the electrical machine and the pump given external limitations such as the needed total dynamic head. Possible matches offer valuable information on possible outflows Q from the pumps and the efficiencies of both, motors and pumps. The difference in performance is mainly caused by the component itself, as well as its subject to external parameters and limitations. With the model offering a list of all motor-pump combinations, it is possible to identify the operation range and the efficiency of each motor-pump set. The selection of the suitable motor-pump unit for this research has been made by focusing on the best subsystem efficiency. However, there are other criteria, that can be used to identify the selected components. The proposed model for the motor-pump unit showed that, depending on the combination of components used together, we can observe a significant difference in operation efficiency. It also showed that, depending on the motor-pump unit, different outflows Q can be satisfied.

To obtain the power supply needed for the motor pump system, a model for the photovoltaic array was introduced. By creating a sample database of different photovoltaic panels with different electrical characteristics, it was possible to investigate the behavior of different photovoltaic panels from different manufacturers when used in solar-powered water pumping systems. The behavior of the photovoltaic subsystem is strongly connected to external influences, such as location. The results showed that, on the one hand, it is possible to implement a reasonable-sized solar-powered water pumping system for Azoia de Baixo in Portugal for the required water demand and pressure height.

On the other hand, implementing the same system with the same framework in Marzling is not feasible and requires a massive oversizing of the photovoltaic array. This is mainly connected to the difference in irradiance that the locations receive, meaning that the irradiance received per year per square meter is significantly higher in the research location in Portugal than in Germany.
However, this study clearly shows that this technology can be a viable option to satisfy the water demand in many locations around the world. Therefore, the usage and optimization of solar-powered water pumps remain a priority to ensure access to fresh water and to reduce greenhouse emissions. The technology offers a reliable and sustainable option for agriculture, as well as for many people in the world who depend on these standalone systems. In general, the results highlighted that the use of solar-powered water pumping systems can never be addressed in a general approach but rather has to be adapted and optimized for each location, influence and limitations. Standalone systems may be a viable solution in some areas but need a complementary power supply elsewhere. Consequently, it is of great importance to consider the environmental framework for the design of a power system.
In conclusion, this study successfully addressed the research question of developing a strategy to optimize the overall performance of solar-powered water pumping systems under diverse environmental conditions by introducing accurate models for the subsystems of the technology to identify the most efficient components during operation. As a result, the study aimed to tailor this approach to specific geographic locations, where it is to emphasize that location and external parameters play a crucial role in the feasibility of power systems.

7.1. Future work

This part aims to give ideas and suggestions that can be used to build on this research. The thesis focuses primarily on the efficiency of individual subsystems and the overall performance of the solar-powered water pumping system. Nevertheless, it may not be of primary interest to the user of the technology to focus on such. As a consequence, the constraints of this work automatically become suggestions for future work.
A very important suggestion for future work is to incorporate a detailed and comprehensive economic evaluation of the different components of the system. This would allow the potential user to select the most economical option for selecting the components.
Another suggestion involves the constraint of the available space. The results of the research were usually automatically those where the least space was occupied. However, in practice space can be a limiting factor. When there is limited space, the sizing of the photovoltaic array becomes the major concern outside of any efficiency and economic observations.
Overall, to create a multidimensional approach, it is necessary to weigh the different constraints against each other.

References

[1] Google Maps.

[2] JRC Photovoltaic Geographical Information System (PVGIS) - European Commission.

[3] I. Bakman. *High-Efficiency Predictive Control of Centrifugal Multi-Pump Stations with Variable-Speed Drives*. 2016.

[4] M. T. Boyd, S. A. Klein, D. T. Reindl, and B. P. Dougherty. Evaluation and validation of equivalent circuit photovoltaic solar cell performance models. *Journal of Solar Energy Engineering, Transactions of the ASME*, 133(2), 2011.

[5] R. Castro. *Electricity Production from Renewables*. Springer International Publishing, 2022.

[6] R. J. Chilundo, U. S. Mahanjane, and D. Neves. Design and Performance of Photovoltaic Water Pumping Systems: Comprehensive Review towards a Renewable Strategy for Mozambique. *Journal of Power and Energy Engineering*, 06(07):32–63, 2018.

[7] A. K. Daud and M. M. Mahmoud. Solar powered induction motor-driven water pump operating on a desert well, simulation and field tests. *Renewable Energy*, 30(5):701–714, 4 2005.

[8] J. A. Duffie and W. A. Beckman. *Solar engineering of thermal processes*. Wiley, 2013.

[9] L. Gevorkov, J. L. Domínguez-García, and L. T. Romero. Review on Solar Photovoltaic-Powered Pumping Systems, 1 2023.

[10] A. A. Ghoneim. Design optimization of photovoltaic powered water pumping systems. *Energy Conversion and Management*, 47(11-12):1449–1463, 7 2006.

[11] C. Ingrao, R. Strippoli, G. Lagioia, and D. Huisingh. Water scarcity in agriculture: An overview of causes, impacts and approaches for reducing the risks, 8 2023.

[12] M. Nabil, S. M. Allam, and E. M. Rashad. Performance improvement of a photovoltaic pumping system using a synchronous reluctance motor. *Electric Power Components and Systems*, 41(4):447–464, 2 2013.

[13] A. Y. Nakhai. Techno-Economic Analysis of a PV-Battery Water Pumping Microgrid System for Off-Grid Rural Communities in the United States: Case Study of the Navajo Nation. Technical report, 2020.

[14] United Nations - Economic and Social Council. Progress towards the Sustainable Development Goals. Technical report, 2022.

[15] B. S. V and S. W. S. Solar photovoltaic water pumping system for irrigation: A review. *African Journal of Agricultural Research*, 10(22):2267–2273, 5 2015.

[16] J. F. Velasco-Muñoz, J. A. Aznar-Sánchez, A. Batlles-delaFuente, and M. D. Fidelibus. Sustainable irrigation in agriculture: An analysis of global research, 2019.

[17] S. Verma, S. Mishra, S. Chowdhury, A. Gaur, S. Mohapatra, A. Soni, and P. Verma. Solar PV powered water pumping system - A review. In *Materials Today: Proceedings*, volume 46, pages 5601–5606. Elsevier Ltd, 2020.

[18] A. W. Kiprono and A. Ibáñez Llario. *Solar Pumping for Water Supply*. Practical Action Publishing, 9 2020.

[19] World Bank Group. Solar Pumping: The basics. 2018.

Table 2: Azoia de Baixo - Results of motor-pump model single phase

Pump Type	Motor Type	Load (%)	η_{Motor}(%)	Q (m^3h^{-1})	P_{Pump} (W)	P_{Motor}(W)	η_{Pump}(%)	$\eta_{Subsystem}$(%)
SP_17	MS 4000	70.11	71.83	3.10	1542.3	2147.3	54.03	38.81

Table 3: Azoia de Baixo - Results of motor-pump model three phase

Pump Type	Motor Type	Load (%)	η_{Motor}(%)	Q (m^3h^{-1})	P_{Pump} (W)	P_{Motor}(W)	η_{Pump}(%)	$\eta_{Subsystem}$(%)
SP7_17	MS 402	70.11	74.91	3.10	1542.3	2058.8	54.03	40.48
SP7_17	MS 4000	70.11	72.08	3.10	1542.3	2139.7	54.03	38.95
SP7_23	MS 4000	95.73	75.08	7.19	2871.8	3825.0	69.07	51.86
SP7_27	MS 4000	84.89	78.24	8.19	3395.7	4340.0	66.82	52.28
SP7_31	MS 4000	95.04	78.08	8.72	3801.8	4869.1	62.94	49.14

Table 4: Azoia de Baixo - Data

Month	$Q/day(m^3/day)$	Hours of operation (h)	$E_{Needed}(kWh)$	Equivalent sun hours (h)	Factor
Jan.	10	1.22	5.40	2.14	2.52
Feb.	15	1.83	8.10	3.47	2.34
Mar.	19	2.32	10.27	4.59	2.24
Apr.	21	2.56	11.34	4.47	2.54
May	33	4.03	17.85	6.77	2.64
Jun.	35	4.27	18,91	7.27	2.60
Jul.	40	4.88	21.61	8.03	2.69
Aug.	33	4.03	17.85	6.78	2.63
Sep.	24	2.93	12,98	5.16	2.51
Oct.	18	2.20	9.74	3.71	2.63
Nov.	10	1.22	5.40	2.21	2.44
Dec.	9	1.10	4.87	1.95	2.50

Table 5: Azoia de Baixo - Results for all panels of database

Panel Name	$\eta_{pv}(\%)$	$\eta_{inv}(\%)$	$\eta_{EM}(\%)$	$\eta_{pump}(\%)$	$\eta_{total}(\%)$	N_{Panel}	P_{Peak} (W)	$A_{Panel}(m^2)$	$A_{Total}(m^2)$
LC50-12M	10.68	98.00	78.24	66.82	5.47	114	5700	0.46	52.50
NU-180	13.54	98.00	78.24	66.82	6.94	32	5760	1.31	41.92
KC200GT	14.03	98.00	78.24	66.82	7.19	29	5800	1.41	40.91
A-255P	15.45	98.00	78.24	66.82	7.92	23	5865	1.62	37.34
A-260P	15.73	98.00	78.24	66.82	8.06	23	5980	1.62	37.34
A-265P	16.05	98.00	78.24	66.82	8.22	22	5830	1.62	35.72
A-270P	16.36	98.00	78.24	66.82	8.38	22	5940	1.62	35.72

Table 6: Marzling - Data

Month	$Q/day(m^3/day)$	Hours of operation (h)	$E_{Needed}(kWh)$	Equivalent sun hours (h)	Factor
Jan.	10	1.22	5.40	1.24	4.36
Feb.	15	1.83	8.10	2.02	4.01
Mar.	19	2.32	10.27	3.58	2.87
Apr.	21	2.56	11.34	5.96	1.90
May	33	4.03	17.85	5.26	3.39
Jun.	35	4.27	18.91	5.16	3.66
Jul.	40	4.88	21.61	6.22	3.47
Aug.	33	4.03	17.85	4.93	3.63
Sep.	24	2.93	12.98	3.90	3.33
Oct.	18	2.20	9.74	1.91	5.10
Nov.	10	1.22	5.40	1.19	4.54
Dec.	9	1.10	4.87	0.77	6.33

Table 7: Marzling - Results for all panels of database

Panel Name	$\eta_{pv}(\%)$	$\eta_{inv}(\%)$	$\eta_{EM}(\%)$	$\eta_{pump}(\%)$	$\eta_{total}(\%)$	N_{Panel}	P_{Peak} (W)	$A_{Panel}(m^2)$	$A_{Total}(m^2)$
LC50-12M	9.31	98.00	78.24	66.82	4.77	677	33850	0.46	311.42
NU-180	11.80	98.00	78.24	66.82	6.05	187	33660	1.31	244.97
KC200GT	13.52	98.00	78.24	66.82	6.93	149	29800	1.41	210.09
A-255P	12.99	98.00	78.24	66.82	6.66	138	33190	1.62	223.56
A-260P	13.11	98.00	78.24	66.82	6.72	137	35620	1.62	221.94
A-265P	13.46	98.00	78.24	66.82	6.90	133	35245	1.62	215.46
A-270P	13.79	98.00	78.24	66.82	7.07	130	35100	1.62	210.6

Table 8: Comparison of results of best system efficiency

System	Panel	$\eta_{pv}(\%)$	$\eta_{inv}(\%)$	$\eta_{EM}(\%)$	$\eta_{pump}(\%)$	$\eta_{total}(\%)$	N_{Panel}	P_{Peak} (W)	$A_{Panel}(m^2)$	$A_{Total}(m^2)$
1	A-270P	16.36	98.00	78.24	66.82	8.38	22	5940	1.62	35.72
2	A-270P	13.79	98.00	78.24	66.82	7.07	130	35100	1.62	210.6